Axial Compression of Three Types of Bamboo Scrimber Columns with Different Cross-sections

Yan Liu,[a] Shukai Tang,[a] Yanfei Guo,[a] Zhongping Xiao,[b,*] and Xiangyu Su [a]

Bamboo scrimber is a versatile material made by rolling and defibering bamboo into loose reticulate bundles (unbroken horizontally, loose longitudinally, and interlaced) that are subjected to drying, gluing, assembling, and hot pressing. In this study, to better understand the application value of bamboo scrimber in construction engineering, the axial compression properties of bamboo scrimber columns with solid, hollow, and I-shaped cross-sections were investigated. For each column type, three lengths of 1 m, 1.5 m, and 2 m (three specimens of each length) were selected and subjected to axial compression testing. The results demonstrated that the primary failure mode of solid bamboo scrimber columns was instability failure, whereas that of hollow and I-shaped columns was mainly debonding failure. Experimental data were further analyzed to better understand and model the failure mechanisms of bamboo scrimber columns. This study led to the establishment of a design formula for bamboo scrimber solid columns, the calculations of which matched well with the experimental results.

Keywords: Bamboo scrimber column; Axial compression; Cross-section structure; Buckling load

*Contact information: a: College of Civil Science and Engineering, Yangzhou University, Yangzhou, Jiangsu 225127, China; b: School of Architectural Engineering Yangzhou Polytechnic Institute, Yangzhou, Jiangsu 225127, China; *Corresponding author: fafuxzp@163.com*

INTRODUCTION

Bamboo is abundant in China, where it ranks second after trees as a forest resource. The quantity and quality of bamboo resources in China rank first in the world. Bamboo scrimber is a type of square-edged timber or board with high specification, large size, and natural bamboo texture. It is made by taking bamboo fiber bundles dried at low temperatures (until their moisture content is below 12%) and subjecting them to the stepwise processes of parallel lay-up, gluing, and hot pressing (or cold pressing), among others. Hence, these loose reticular bamboo fiber bundles are long and cross-linked, yet they retain the original arrangement of fibers. This confers several advantages to bamboo scrimber, which include a high bamboo utilization rate, excellent physical and mechanical properties, a beautiful appearance, and a low cost with good economic benefits. Currently, domestic bamboo scrimber is used mainly in indoor and outdoor flooring, enclosure structures, and veneers and furniture making, but it is rarely used in building structures in China. How to apply bamboo to architectural structure is a research topic that has just begun. Based on a search of the literature, it was found that there has been a lack of research on the performance of bamboo scrimber columns in building structures.

Zhang *et al.* (2015) conducted axial compression tests on four bamboo scrimber columns with a square cross-section and found ultimate load-carrying capacities that were close to the theoretical calculated values. Su *et al.* (2015) concluded that the primary failure mode of the axial compression of bamboo scrimber columns is ductile failure, and the

failure forms consisted of the strength failure of end-crushing and instability failure of the tensile side of the middle span accompanied by fiber breaking; this led to a model formula for calculating the ultimate capacity of bamboo scrimber columns under axial compression. In other work, axial compression test results for Glulam columns with different slenderness ratios were compared with domestic and foreign codes (Xiao *et al.* 2015). In addition, a study of 50 axially loaded wood scrimber columns with different slenderness ratios provided the theoretical and experimental basis for the engineering application of wood scrimber (Li *et al.* 2015). Work by Li *et al.* (2015) made important contributions to the understanding of the mechanical properties of bamboo scrimber under axial loading. For example, their research examined the axial compression properties of short columns with different slenderness ratios made from different parts of bamboo (Li *et al.* 2013, 2015a,b). Through using lateral-pressure-glued laminated bamboo columns to perform eccentric compression tests, Li *et al.* (2015) found that the joint and slub parts were the weakest part of the tensile zone, and the mean strain value of the mid-span section was consistent with the value calculated from the plane-section. Based on this work, they derived a formula to calculate the eccentric cross-section bearing capacity for use in a stress-strain model under compression of glued laminated bamboo columns (Li *et al.* 2016a,b). A method of calculating the eccentricity bearing capacity of bamboo scrimber columns was recently proposed by Wei *et al.* (2016). Previously, Luna *et al.* (2013) drew a critical slenderness ratio diagram by studying the mechanical properties of bamboo scrimber columns with solid and hollow sections under different slenderness ratios.

In summary, previous domestic and foreign research typically used only solid sections when testing the axial compression of bamboo scrimber columns. Because the volume-weight of bamboo scrimber is large, hollow sections, I-shaped sections, and different column heights were also investigated in this study. Therefore, the axial compressive performance of each section under varied slenderness ratios was compared to expand the application potential of bamboo scrimber columns for building structures. The research work of this paper entails a certain degree of pioneering.

EXPERIMENTAL

Design of Specimen

A total of 27 bamboo scrimber column specimens were provided by the Jiangxi Chunhong Bamboo Technology Co., Ltd. (Jiangxi, China). These specimens were made from 5-year-old bamboo *via* cold pressing and splicing. A phenolic resin was used as the adhesive used for cold pressing, and the splice glue was a single component, moisture-cure polyurethane adhesive. Figure 1 shows the cross-sectional sizes. Three specimen heights were also considered in the tests: 1 m, 1.5 m, and 2 m, each of which was replicated with three specimens per specification (solid, hollow, and I-shape) for a total of 27 specimens. As described in Table 1, these experimental specimens were labeled as SXZ1-1~SXZ3-3, KXZ1-1~KXZ3-3, and GZZ1-1~GZZ3-3 according to their treatment combinations. The section size and test piece of bamboo scrimber columns are shown in Figs. 1 and 2, respectively, as described earlier by Su (2017).

Before axial compression testing, the physical and mechanical properties of the bamboo scrimber specimens were determined. The bamboo scrimber had an air-dried density of 1.204 g/cm^3, an average moisture content of 6.6%, a compressive strength along the grain of 57.4 MPa, a standard compressive strength along the grain of 55.5 MPa, an

elastic modulus along the grain of 1180 MPa, and a Poisson ratio of 0.384.

Table 1. Specimens of Bamboo Scrimber Columns for Axial Compression Testing

Section Forms	Specimen Group Labels	Height of Specimens (mm)	No. of Specimens
Solid Columns	SXZ1-1~SXZ1-3	1000	3
	SXZ2-1~SXZ2-3	1500	3
	SXZ3-1~SXZ3-3	2000	3
Hollow Columns	KXZ1-1~KXZ1-3	1000	3
	KXZ2-1~KXZ2-3	1500	3
	KXZ3-1~KXZ3-3	2000	3
I-shaped Columns	GZZ1-1~GZZ1-3	1000	3
	GZZ2-1~GZZ2-3	1500	3
	GZZ3-1~GZZ3-3	2000	3

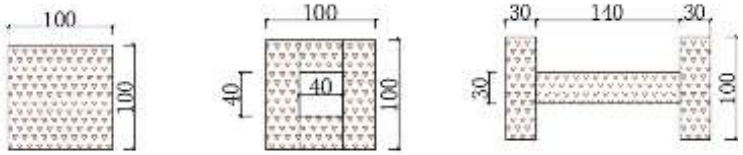

Fig. 1. Sectional dimensions of bamboo scrimber specimens: (a) Solid section; (b) Hollow section; (c) I-shaped section (This information appeared earlier in (Su 2017)

Fig. 2. The specimens used for axial compression of bamboo scrimber columns

Experimental Measurements and Loading

The experiment was conducted in the structural laboratory of the College of Civil Engineering of Yangzhou University in Yangzhou, Jiangsu, China. The loading system and test process followed GB/T 50329 (2013), GB 50005 (2017), and ASTM D198-15 (2015). A YAJ-5000 microcomputer (Changchun Kexin Test Instrument Co., Ltd., Changchun, China) controlled the electro-hydraulic servo test machine to perform axial loading on the study specimens. The experiment consisted of four main steps:

(1) Marking the four surfaces of a specimen clockwise as A, B, C, and D.

(2) Pasting two strain gauges to each surface of the specimens along the grain (parallel to column length) and cross-grain (perpendicular to column length).

(3) Adjusting the positions of two end-knife hinge supports and the specimens to ensure their geometric alignment and then affixing dial indicators midway onto the top of surface-A and the top, middle, and bottom parts on surface-B of the column.

(4) Using a force control method to complete the step loading applied to each specimen. The loading time was controlled within 15 min, and the loading rate was 2000 N/s. When the loading value of each stage was reached, the resistance strain gauge and percentile meter readings were recorded, and the experimental phenomena were observed (with photographs and records as required).

Figure 3, as published by Su (2017), shows the layout of the test device and measurement points. To ensure the safety of all tests, a safety net was attached around the column-testing machine, as shown in Fig. 4.

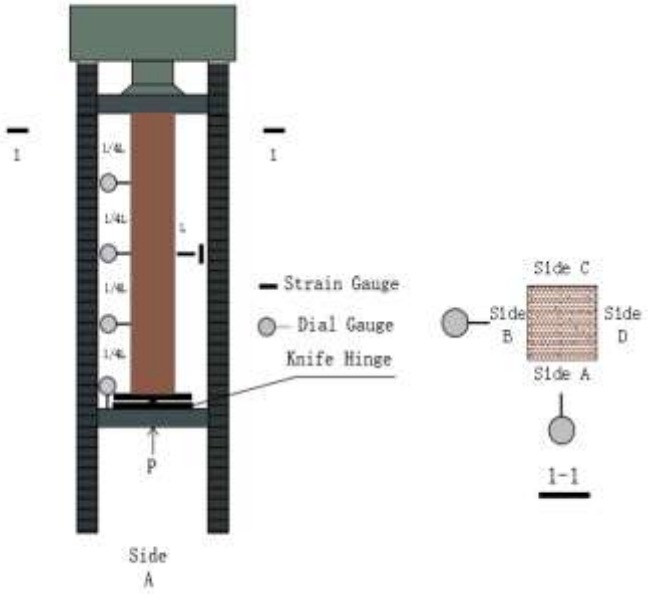

Fig. 3. The layout of the measuring points on the bamboo scrimber columns (This diagram appeared earlier in (Su 2017).

Fig. 4. The test device used for axial compression testing

RESULTS AND DISCUSSION

Failure Mode of the Bamboo Scrimber Columns

The experimental and failure phenomena of the specimens with solid, hollow, and I-shaped sections clearly differed, but the failure phenomena of specimens with the same cross-sections and different lengths were similar.

Specimens with solid sections did not appear to undergo strength failure, but they underwent overall instability failure. At the initial stage of loading, no obvious changes were observed. When the specimen was loaded to 0.7 P_u to 0.8 P_u, the dial data slowly increased, and a slight jump in the strain gauge reading occurred, which showed that deformation had increased despite the no-load increase and strength failure in the specimen.

With continued loading, the specimen surface bulged slightly, and the finger joint cracked slightly. When loaded to 0.9 P_u, the specimens underwent slight lateral bending. When the loading approached the P_u of the specimens, the flexure deformation of the specimens became intensified, and buckling suddenly occurred. The typical failure phenomena of the solid column specimens are shown in Fig. 5a.

The failure phenomena of the hollow columns were mainly degumming and bursting apart. When loaded to 0.9 P_u, the specimen bent slightly. As the load continued to increase, the degree of deflection suddenly intensified. Shortly after, the specimen disintegrated from the column center into four pieces of bamboo scrimber plates, which was accompanied by a loud sound. Cracks spread rapidly along the adhesive bonding surface to the end of the column until the specimen disintegrated completely. The typical failure phenomena of the hollow column specimens are shown in Fig. 5b.

The failure phenomena of the I-shaped column were mainly degumming and cracking. When loaded in the range 0.7 P_u to 0.8 P_u, the dial data slowly increased, and the strain gauge reading jumped slightly. With further loading, the specimen's exterior bulged slightly, and the finger joint cracked slightly. With even further loading, the flexural degree of the specimens slowly increased. When the loading was near the P_u of the specimens, the web and flange plates suddenly degummed, which made a dull "peng" sound. The flange plates were degummed and cracked in the direction perpendicular to the previous flexural direction. After flange plate degumming, the web underwent a large deflection suddenly, and then destabilization occurred. The typical failure phenomena of the I-shaped specimens are shown in Fig. 5c.

(a) **(b)** **(c)**

Fig. 5. Failure modes of the bamboo scrimber columns: (a) Solid column; (b) Hollow column; (c) I-shaped column

Test Results of Bamboo Scrimber Columns Under Axial Compression

The test results of the bamboo scrimber columns under axial compression are summarized in Table 2, in which the section area and ultimate load are mean values of three replicate specimens in the same cross-section group. The ultimate load was lower when the specimens had a higher slenderness ratio. For the same slenderness ratios, the ultimate load of the solid columns was higher than those of both the hollow and I-shaped columns. During the test, the ultimate bearing capacity of the three specimens within the same group displayed some discreteness. The reasons for this observation are detailed below.

Bamboo scrimber is a type of artificial bamboo plank made from pressed bamboo

fiber by dipping in glue after silk cutting. The fineness of a bamboo fiber determines the size of the dipping area, and the pre-existing uniformity of the bamboo fiber layer determines the uniformity of the bamboo board. The bamboo fiber layer's strength is determined by the infiltration of the adhesive into the bamboo filaments. Therefore, even though the bamboo scrimbers were produced in the same batch, they were some slight differences among them. Further, when columns needed to be lengthened, the different positions of the finger joints may have also caused changes in bearing capacity. Due to the randomness of the joint position, there were some differences in the bearing capacity of specimens within the same batches.

Table 2. Test Results of the Specimens Under Axial Compression

Specimens	Slenderness Ratio (λ)	Section Area (A, (mm^2))	Ultimate Load P_u (KN)
SXZ1-1~SXZ1-3	34.65	10008.48	564
SXZ2-1~SXZ2-3	51.97	10010.33	446
SXZ3-1~SXZ3-3	69.30	9993.69	337
KXZ1-1~KXZ1-3	32.16	8403.47	455
KXZ2-1~KXZ2-3	48.25	8411.38	408
KXZ3-1~KXZ3-3	64.33	8399.10	234
GZZ1-1~GZZ1-3	43.81	10202.77	490
GZZ2-1~GZZ2-3	65.71	10119.76	348
GZZ3-1~GZZ3-3	87.61	10174.43	222

Load–axial Displacement Curve of Bamboo Scrimber Columns

Figure 6 shows the load–axial displacement curves of the solid, hollow, and I-shaped bamboo columns with different slenderness characteristics, in which the values of each curve are the average of three samples (likewise for following curves presented).

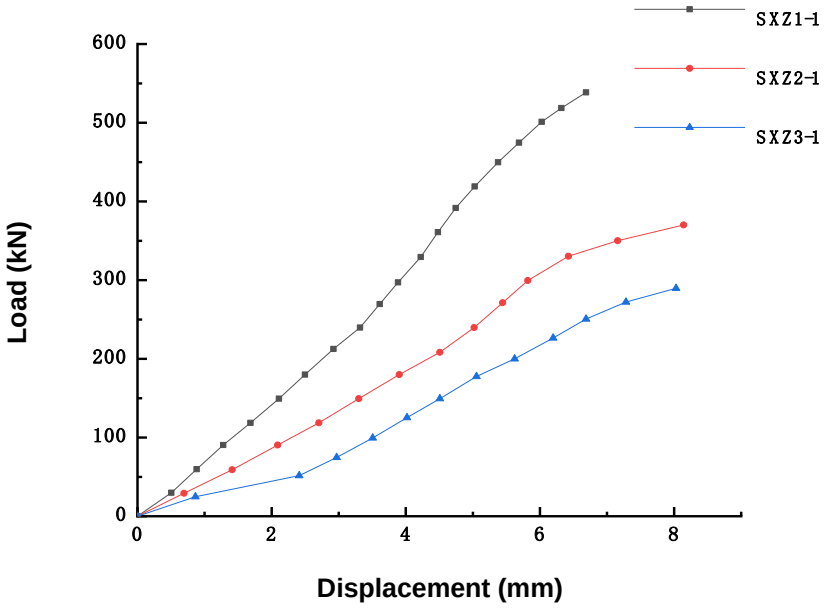

(a)

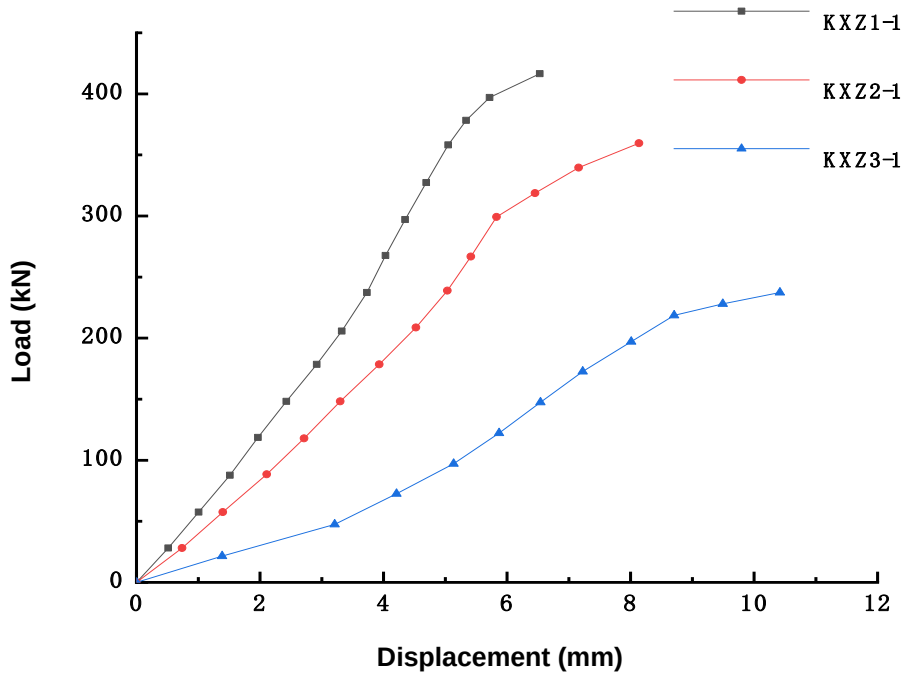

(b)

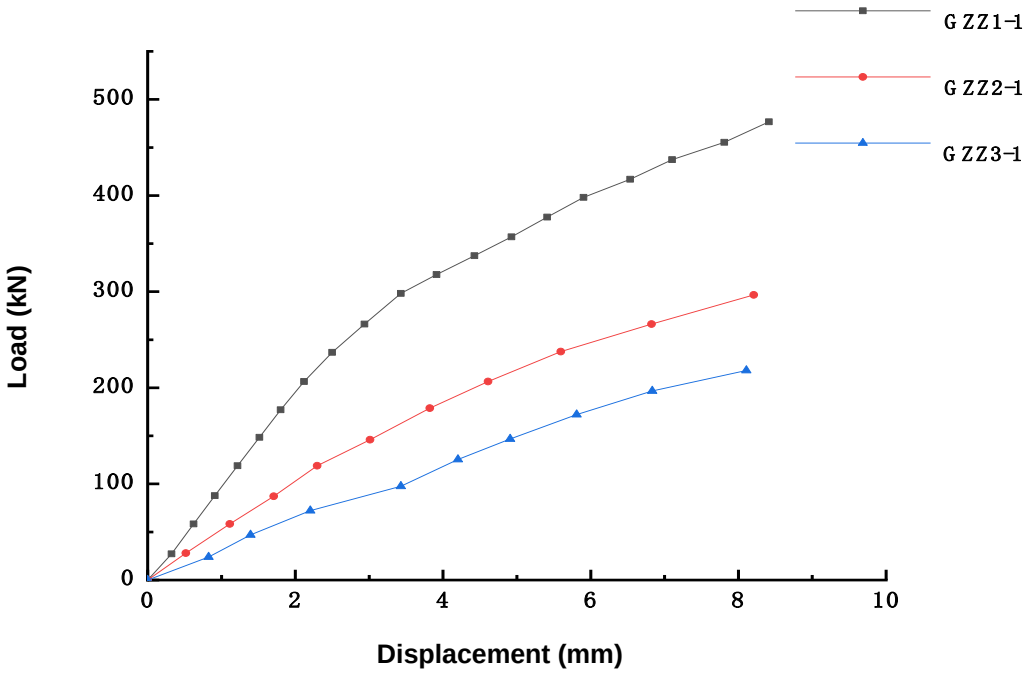

(c)

Fig. 6. Load–axial displacement curves: (a) Load-axial displacement curve of solid bamboo scrimber columns; (b) Load-axial displacement curve of hollow bamboo scrimber columns; (c) Load-axial displacement curve of I-shaped bamboo scrimber columns

The curve can be divided into two stages. The first stage was the elastic stage. When the load was approximately 0 to 0.4 P_u, the curve was a straight line, and the specimen was elastic. The second stage was the elastic-plastic stage. When the load exceeded 0.4 P_u and continuously increased, the slope of the curve gradually decreased, which indicated that the specimen exhibited elastic-plastic behavior. According to Fig. 6, the initial stiffness of the specimens decreased as slenderness ratio increased. Because of the sudden brittle failure of the specimens, the axial deformation values of the three groups of specimens were not large.

Load–transverse Deflection Curve of Bamboo Scrimber Columns

The load-transverse deflection curves of the solid, hollow, and I-shaped specimens with three heights are shown in Fig. 7. In the initial stage of loading, as the load increased, the transverse deformation of solid column specimens increased marginally, whereas the transverse deformation of the hollow and I-shaped specimens all increased.

When the solid column was loaded to approximately 0.8 P_u, the slope of the P-δ curve suddenly decreased, and the lateral deflection increased abruptly. Subsequently, although the load did not increase greatly, the out-of-plane deflection of the specimens continued to increase, and localized swelling and crushing occurred in the solid specimen. The failure of the solid columns was mainly caused by instability. When the hollow and I-shaped columns were loaded to approximately 0.7 P_u, the slope of the P-δ curve decreased, and the lateral deformation began to increase remarkably. Thereafter, although the load did not increase remarkably, the lateral deflection of the specimens continued to increase. This may have been due to the second-order effect of the initial eccentricity in the specimens. Finally, degumming and separating between the plates occurred in both kinds of column specimens, and the specimens lost their integrity and were damaged as a result.

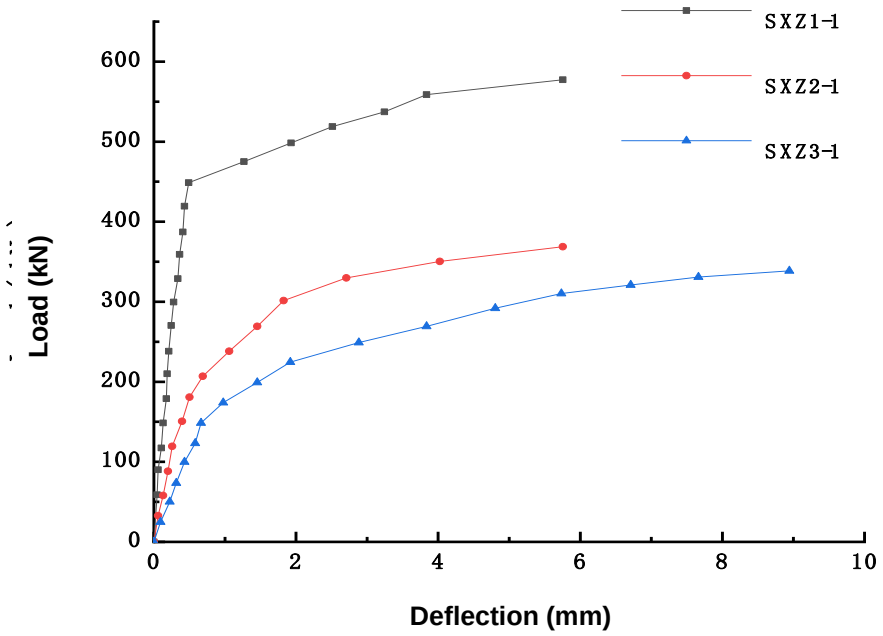

(a)

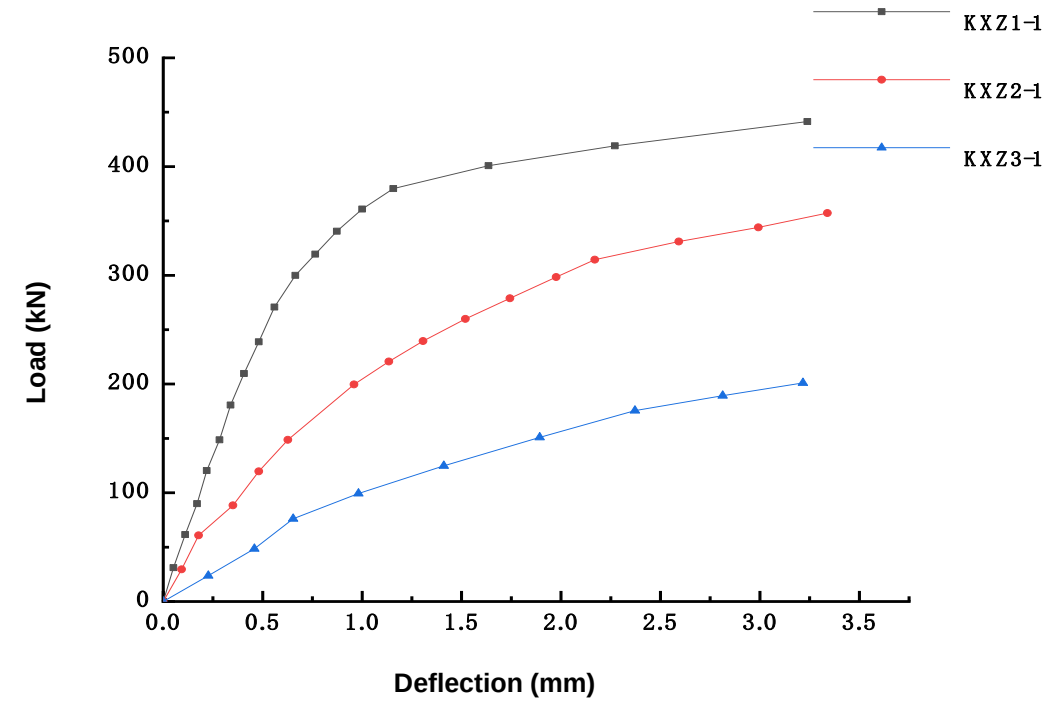

(b)

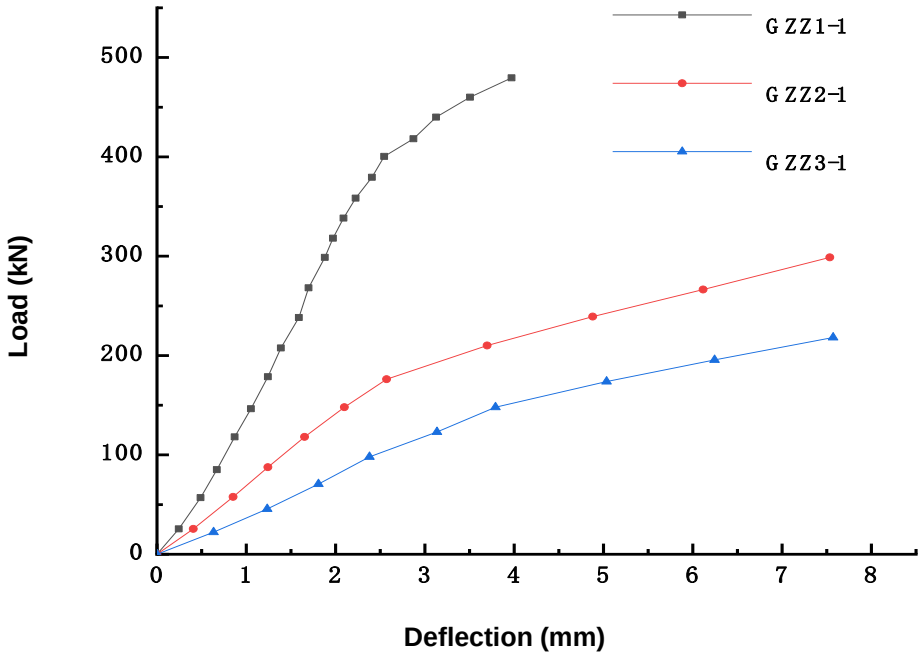

(c)

Fig. 7. Load–transverse deflection curves: (a) Load-transverse curve of solid bamboo scrimber columns; (b) Load-transverse curve of hollow bamboo scrimber columns; (c) Load-transverse curve of I-shaped bamboo scrimber columns

Load–longitudinal Strain Curve of Bamboo Scrimber Columns (*P-ε* Curve)

Figure 8 shows the typical load–longitudinal strain curve of the solid, hollow, and I-shaped specimens of 2.0 m in height.

For solid columns, at the initial stage of loading, the *P-ε* curves of the four surfaces per specimen were straight lines, and their values were the same, which indicated that the specimens were in the elastic stage and under axial compression. However, when the load reached approximately 0.8 P_u, as the slenderness ratio increased, the *P-ε* curves of the four surfaces began to diverge. One of the surface strains decreased remarkably, whereas the relative surface strains increased. This result indicated that the specimen underwent transverse deformation, which indirectly confirmed the occurrence of the deformation of the solid columns described earlier.

For the hollow and I-shaped columns, at the initial stage of loading, the specimens were in an elastic stage, as the *P-ε* curves of the four surfaces were parallel but their strain values differed. Under loading of approximately 0.6 P_u, as the slenderness ratio increased, the slope of the curves diminished, and the strain differential among the four surfaces increased; thus, the stress upon each plate was also unequal. This result this may have been due to the sensitivity of the hollow and I-shaped cross-section specimens to initial eccentricity, and the second-order effect may have led to unequal strains and stresses of the plates at different positions in the columns. Hence, under the action of axial pressure, the plates may have undergone lateral deformation that generated horizontal stress in the bond layers. When the direction of the lateral deformation was parallel to the bond layers, this horizontal stress is shear stress, and when vertical to the bond layer, the horizontal stress was tensile stress. Further, with greater loading, the bonding force between plates was insufficient to resist the horizontal stress produced. When the first degummed plate separated from the main body, the force on the remaining part became more uneven, which degummed the whole section until it suddenly burst apart.

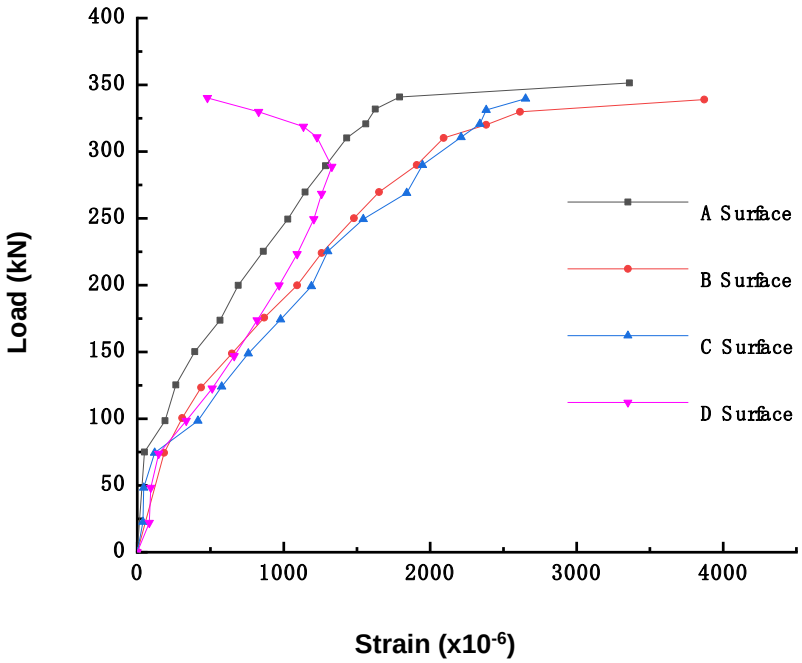

(a)

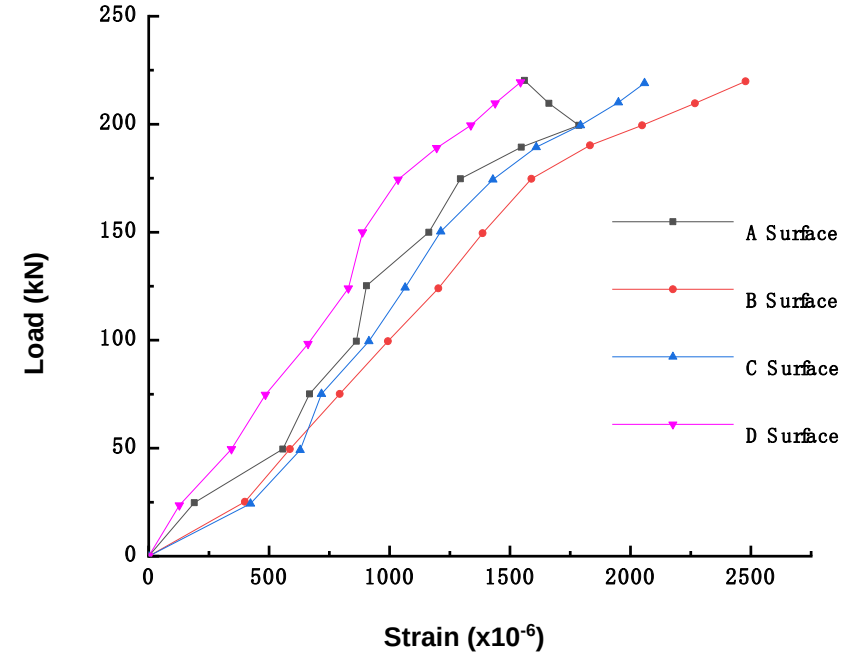

(b)

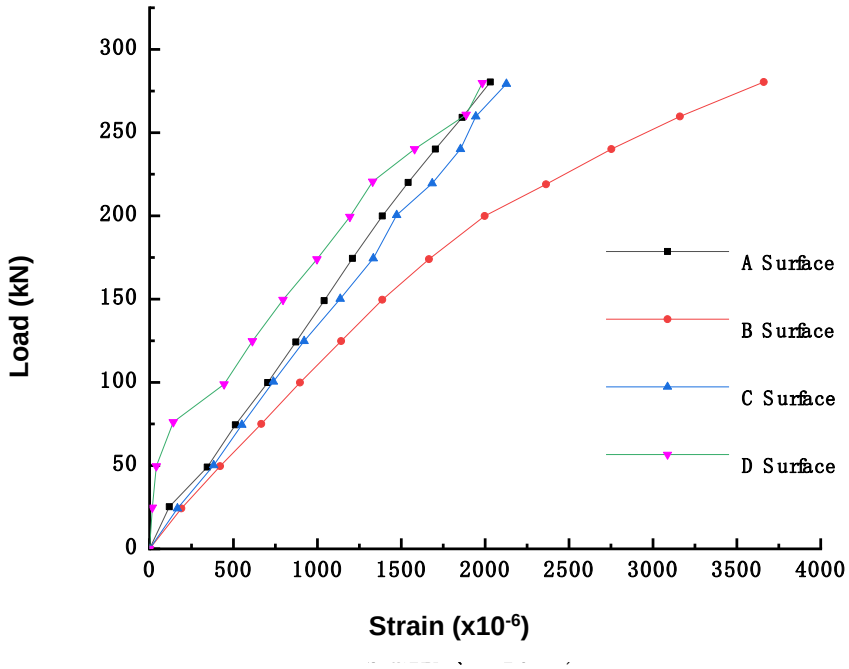

(c)

Fig. 8. Load–longitudinal strain curves: (a) Load-longitudinal strain curve of solid bamboo scrimber columns; (b) Load-longitudinal strain curve of hollow bamboo scrimber columns; (c) Load-longitudinal strain curve of I-shaped bamboo scrimber columns

The above analysis shows that, because of the second-order effect, the longitudinal strain values of each plate in the hollow and the I-shaped bamboo columns were different at the later stage of loading. Consequently, there was randomness to the degumming that occured in the bond area and to the failure position of the hollow and I-shaped columns. In contrast, the strain upon each section of the solid column specimens was relatively uniform at the later stage of loading, and their load-bearing capacity and reliability were better than those of the hollow or I-shaped column specimens.

Theoretical Analysis

The ultimate bearing capacity (P_u) measured was compared with the calculated value of the ultimate bearing capacity (P_c) based on the current Chinese code for the Design of Timber Structure (hereafter referred to as the GB 5005 (2003)), as shown in Table 3 and Fig. 9. This allowed for the exploration of the applicability of the "timber code" to bamboo scrimber columns.

Term 5.1.2 of the "timber code" gives the equations for calculating the bearing capacity of axially compressed members according to stability checking. Term 5.1.4 gives the equations for calculating the stability coefficient φ of axially-compressed members according to the strength grades of different tree species.

The equation for the bearing capacity of axially-compressed members according to stability is as follows (Eq. 1),

$$\frac{N}{\varphi A_0} \leq f_c \quad (1)$$

where N is the axial pressure (kN), f_c is the design value of compressive strength along the grain, and A_0 is the total cross-sectional area (m^2).

For those tree species whose intensity grades are TC15, TC17, and TB20, the φ was calculated as follows (Eq. 2 and Eq. 3),

$$\text{when } \lambda \leq 75, \quad \varphi = \frac{1}{1+\left(\frac{\lambda}{80}\right)^2} \quad (2)$$

$$\text{when } \lambda > 75, \quad \varphi = \frac{3000}{\lambda^2} \quad (3)$$

where λ is the slenderness ratio.

Correspondingly, for tree species whose intensity grades are TC11, TC13, TB11, TB13, TB15, and TB17, φ was calculated as follows (Eqs. 4 and 5):

$$\text{when } \lambda \leq 90, \quad \varphi = \frac{1}{1+\left(\frac{\lambda}{65}\right)^2} \quad (4)$$

$$\text{when } \lambda > 90, \quad \varphi = \frac{2800}{\lambda^2} \quad (5)$$

However, because there was no gap in construction, $A_0 = A$. The value of λ was calculated by Eq. 6 and Eq. 7,

$$\lambda = \frac{l_0}{i} \tag{6}$$

$$i = \sqrt{\frac{I}{A}} \tag{7}$$

where l_0 is the calculation length of the specimen and l is the length of the specimen, but when the specimen the hinged at both ends, $l_0=l$; i is the rotation radius (m) of the specimen section, and I is the full-section moment of inertia of the specimen.

By comparing the compressive strength, parallel shear strength, and elastic modulus of the bamboo scrimber reported in Su *et al*. (2017) and Tables 3 in GB 5005 (2003), the mechanical property of the bamboo scrimber was found to approximate a grade of TB20. Therefore, Eq. 3 was used to calculate the stability of its axially compressed specimens, according to GB 50005 (2003). Below is the equation for calculating the ultimate bearing capacity (Eq. 8),

$$P_c = \varphi f_k A \tag{8}$$

where f_k is the standard value of compressive strength along the grain (MPa), and A is the cross-sectional area (m^2) of the bamboo scrimber column.

Most of the experimental values exceeded the calculated values, and the greatest difference was found for the columns of 1 m in height (Table 3 and Fig. 9). The experimental value of the hollow columns with a height of 2 m was slightly lower than the value calculated from the equation. As the slenderness ratio increased, the experimental and calculated values became more similar.

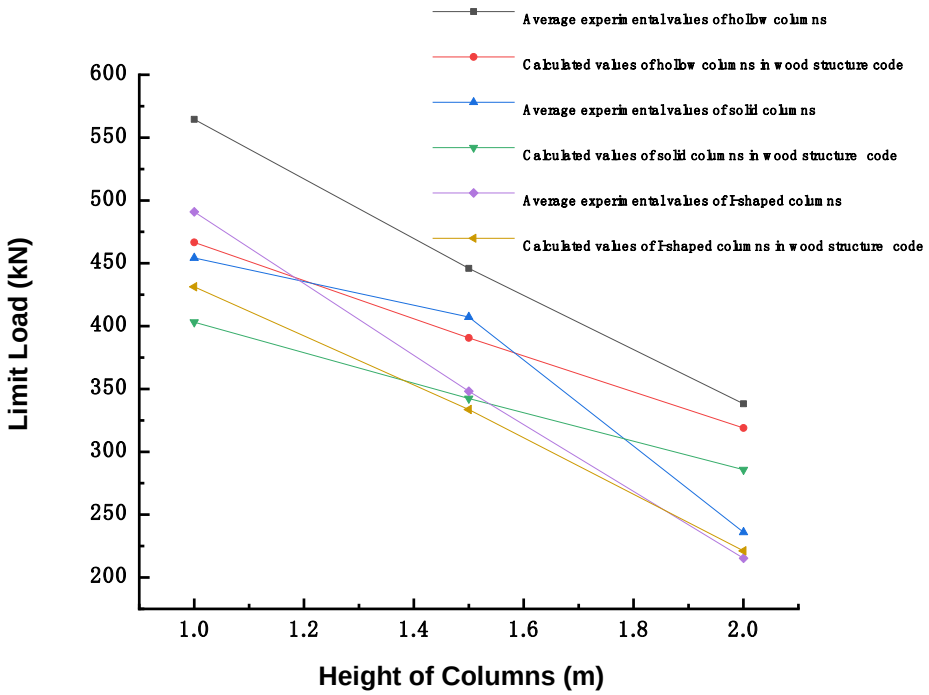

Fig. 9. Comparison of the experimental and predicted values of the bamboo scrimber specimens

Table 3. Comparison of the Tested and Calculated Values of the Specimens

Specimens	P_u* (KN)	φ_c	P_c (KN)	$\frac{P_U - P_C}{P_C}$ %
SXZ1-1~SXZ1-3	564	0.84	468	20.63
SXZ2-1~SXZ2-3	446	0.70	390	14.18
SXZ3-1~SXZ3-3	337	0.57	316	6.3
KXZ1-1~KXZ1-3	455	0.86	400	13.46
KXZ2-1~KXZ2-3	408	0.73	342	19.35
KXZ3-1~KXZ3-3	235	0.61	283	-17.06
GZZ1-1~GZZ1-3	490	0.76	432	15.75
GZZ2-1~GZZ2-3	348	0.60	335	3.92
GZZ3-1~GZZ3-3	252	0.39	220	14.44
*Note: P_u is the average value of three specimens tested in the same group.				

Designing Formulae for Solid Bamboo Scrimber Columns

The experimental results showed that the failure modes of the solid columns were mainly buckling and instability, whereas the hollow and I-shaped columns were mainly degummed. Because the stress on the plates in the hollow and the I-shaped columns did not reach the ultimate strength, the structural design and configuration should be strengthened for the hollow and I-shaped bamboo scrimber columns. Before deducing such a bamboo-specific equation, the failure mechanism of the bamboo scrimber column is discussed.

For solid columns, the ultimate bearing capacity of the specimens was affected by the finger joint. At present, the maximum length of bamboo scrimber sheets produced by domestic production lines is 1.83 m. The positions of finger joints were in a random distribution, and they constituted the weakest part of the bamboo scrimber columns. When the slenderness ratio of the specimen was small, the internal forces of the specimens were more uniform, and their failure conformed to the stability theory of the compression bar. For the specimens with high slenderness ratios, the influence of finger joints was larger, as the skin of the columns bulged and cracked near the finger joints. This resulted in a reduction in the section inertia moment of the specimen. As the slenderness ratio increased, the bearing capacity of the bamboo scrimber columns was reduced. Bending fracture may occur when the resistance of the specimen is less than the axial compressive stress.

For the hollow columns, the ultimate bearing capacity of specimens was affected by adhesive viscosity. The hollow columns were made of four finished sheets bonded by one-component moisture-cure polyurethane adhesive. In the early stage of loading, the resistance of the specimen was sufficient to bear the external force applied. When the load approached its maximum, a horizontal force caused by the load between the glued surfaces of the plate exceeded the bond force of the glued layer, and then degumming occurred. The weakest plates became unglued and separated first, which resulted in a loss of specimen integrity and the failure of the specimen to carry the load. The other three plates of the remaining part of the specimen were degummed and separated rapidly. These specimens often burst during breaking.

For the I-shaped specimens, the bearing capacity was also affected by the adhesive viscosity. The weak inertia axis of the I-column was parallel to the web direction. With an increased axial load, the I-column deflected perpendicularly to the web, and the web deflected more severely than the flange plates. Torque and horizontal shear force were thus produced at the mid-span bonding of the web and the flange plate. When the shear stress

exceeded the adhesive force, the web and flange degummed, the I-shaped specimen separated from the whole into three plates, and the specimen was fractured.

Combined with the test results, the above equations of the Timber Code were revised accordingly with new formulas to calculate the ultimate compressive strength for solid bamboo scrimber columns. Referring to the findings of Luna *et al*. (2013), the concept of critical slenderness ratio was introduced, which was defined as '$\lambda_0 = 50$'.

Because the axial compressive properties of bamboo columns with a large slenderness ratio are greatly affected by the finger joint, when the slenderness ratios of the specimens exceed 50, the adverse effects of the finger joints should be considered. Through analysis and comparison with the test results, the formula for calculating the ultimate bearing capacity of solid bamboo scrimber columns was obtained as follows (Eq. 8),

$$P_k = \begin{cases} \dfrac{f_{ck}A}{1+\left(\dfrac{\lambda}{80}\right)^2} & (\lambda \le 50) \\ \dfrac{2100}{\lambda^2} f_{ck}A & (\lambda > 50) \end{cases} \quad (8)$$

where P_k is the calculation value of ultimate bearing capacity (kN), and f_{ck} is the standard value (MPa) of compressive strength along the grain of solid bamboo scrimber columns; the other parameters are the same as defined for the previous equations.

The ultimate bearing capacities of the solid bamboo scrimber columns with heights of 1.0 m, 1.5 m, and 2.0 m were calculated by Eq. 8 and compared with the averaged test values from the experiment (Table 4).

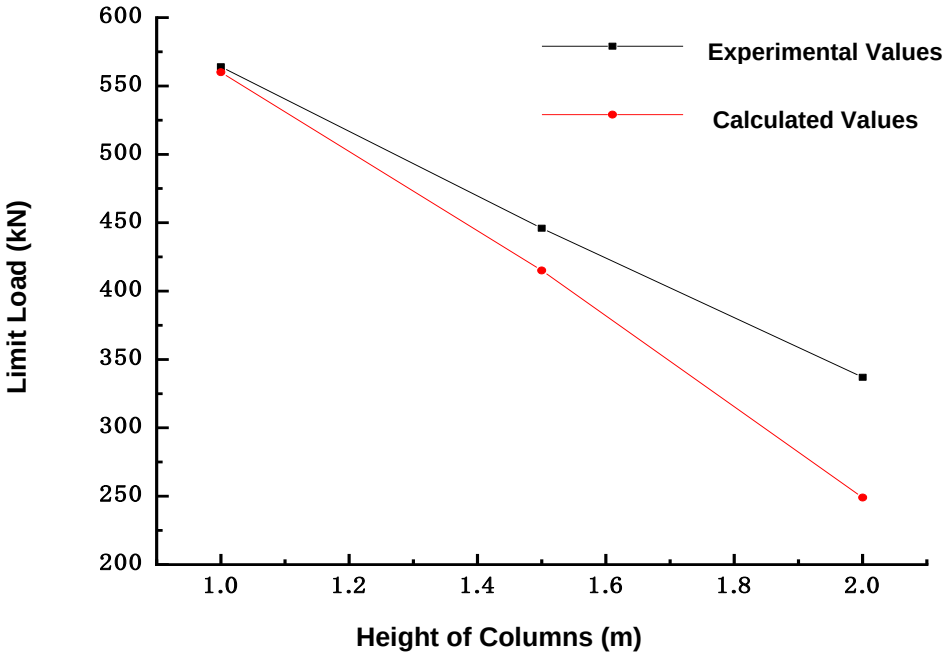

Fig. 10. Comparison of experimental values for the solid columns and the predicted values from the design formula

Table 4 shows that Eq. 8 better captured the true bearing capacity of the solid bamboo columns with small slenderness ratios and reserved enough safety factor when the slenderness ratio was large. As Fig. 10 shows, the experimental values of the 1.0 m-high and 1.5 m-high solid columns almost matched the formula's predicted values. However, the 2.0 m-high solid column formula gave a value slightly smaller than the observed value, and its safety factor was higher.

Table 4. Comparison of Experimental Values and the Values Calculated from the Designed Formula

Specimens	P_u (KN)	P_k (KN)	$\frac{P_U - P_k}{P_k}$ %
SXZ1-1~SXZ1-3	564	560	0.71
SXZ2-1~SXZ2-3	446	415	7.47
SXZ3-1~SXZ3-3	337	249	35.34

CONCLUSIONS

1. The main failure mode of the bamboo scrimber solid columns was instability failure, and the failure modes of the bamboo scrimber hollow columns and I-shaped columns were mainly due to glue failure. The ultimate strengths of the hollow and I-shaped columns were limited by the bond strength of their structures; constrained by the bond strength, the specimens could not make the best of the high compressive strength of bamboo scrimber. With higher slenderness ratios, the ultimate bearing capacity of the bamboo scrimber columns decreased rapidly.
2. As the slenderness ratio increased, the ultimate strength of the bamboo scrimber columns decreased more quickly than predicted by GB 50005 (2017), which showed that the influences of finger joints and adhesives should not be ignored when considering the bearing capacity of full-scale bamboo scrimber columns. In this paper, the calculation formula of the ultimate compressive strength of solid bamboo scrimber columns was revised, and novel formulas were developed that are likely more reliable.
3. The gluing area of the hollow and I-shaped columns was much smaller than that of the solid columns, which caused the primary failure mode of the specimens to occur *via* de-gluing, as the buckling of these specimens under compression was not obvious. Because the sizing and finger joints were weak points of force, fixing measures should be added to the hollow and I-shaped columns to increase their overall stiffness. The addition of fixing measures would utilize the high strength of the materials made with bamboo scrimber.

AKNOWLEDGMENTS

The authors thank the National Science Foundation of China and Ministry of Science and Technology of China. This research was funded by the National Science Foundation of China in 2019 (Grant No. 51878590) and National Key Research and Development Program in 2017 (Grant No. 2017YFC0703505).

REFERENCES CITED

ASTM D198-15 (2019). "Standard test methods of static tests of lumber in structural sizes," ASTM International, West Conshohocken, PA, USA.

GB 50005 (2003). "Code for design of timber structure," China Architecture & Building Press, Beijing, China. (In Chinese)

GB/T 50329 (2012). "Standard for test methods of timber structures," China Architecture & Building Press, Beijing, China. (In Chinese)

Li, H.-T., Zhang, Q.-S., Huang, D.-S., and Deeks, A. J. (2013). "Compressive performance of laminated bamboo," *Composites Part B: Engineering* 54(1), 319-328. DOI: 10.1016/j.compositesb.2013.05.035

Li, H. T., Zhang, Q., and Wu, G. (2015a). "Stress-strain model of side pressure laminated bamboo under compression," *Journal of Southeast University* 45(6), 1130-1134. (In Chinese) DOI: 10.3969/j.issn.1001-0505.2015.06.019

Li, H.-T., Su, J.-W., Zhang, Q.-S., Deeks, A. J., and Hui, D. (2015b). "Mechanical performance of laminated bamboo column under axial compression," *Composites Part B: Engineering* 79, 374-382. DOI: 10.1016/j.compositesb.2015.04.027

Li, Z., He, M., Tao, D., and Li, M. (2016a). "Experimental buckling performance of scrimber composite columns under axial compression," *Composites Part B: Engineering* 86, 203-213. DOI: 10.1016/j.compositesb.2015.10.023

Li, H.-T., Wu, G., Zhang, Q.-S., and Chen, G. (2016b). "Experimental study on side pressure LBL under tangential eccentric compression," *Journal of Hunan University* 43(5), 90-96. (In Chinese)

Li, H., Wei, D., Su, J., Yuan, C., and Chen, G. (2016c). "Experimental study on PSBL under eccentric compression," *Journal of Building Materials* 19(3), 561-564, 583. (In Chinese) DOI: 10.3969/j.issn.1007-9629.2016.03.025

Luna, P., Takeuchi, C., Alvardo, C., and Moreno, I. (2013). "Glued laminated *Guadua angustifolia* bamboo columns," *Acta Horticulturae* 1003, 125-130. DOI: 10.17660/ActaHortic.2013.1003.16

Su, J. W., Wu, F., Li, H., and Yang, P. (2015). "Experimental research on parallel bamboo strand lumber column under axial compression," *China Sciencepaper* 10(1), 39-41. (In Chinese)

Su, X. Y. (2017). *A Study on the Axial Behavior of Bamboo Scrimber Columns with Three Different Cross-sections*, Yangzhou University, Yangzhou, China. (In Chinese)

Wei, Y., Zhou, M. Q., and Yuan, L. (2016). "Eccentric compressive properties of bamboo scrimber columns," *Journal of Composites* 33(2), 379-385. (In Chinese)

Xiao, Y., Feng, L., Lv, H. G., She, L. Y., Shen, Y. L. (2015). "Experimental studies of glubam columns under axial loads," *Industrial Construction* 45(4), 13-17. (In Chinese)

Zhang, S., Zhao, Z., Zhang, W., and Shi, Y. (2015). "Experimental research on axial compression of recombinant bamboo columns," *Construction Technology* 44(24), 120-123. (In Chinese)

Article submitted: May 21, 2020; Peer review completed: August 15, 2020; Revised version received: August 19, 2020; Accepted: August 31, 2020; Published: September 7, 2020.
DOI: 10.15376/biores.15.4.8093-8109